ed, the tibia is typically shorter than the femur (crural index <100), and the metapodials are relatively short (femorometatarsal index <50). They appear considerably more generalized than *Diacodexis*.

The crural and femorometatarsal indices tend to be highest in running (cursorial) and jumping (saltatorial) mammals. The crural index for *Diacodexis* reflects such habits, falling in the middle of the range for living ruminants as well as that for rabbits (*29*). The femorometatarsal index is extraordinarily high for an early Eocene mammal and is comparable to that in many extant ruminants and higher than in rabbits (*29*). Thus *Diacodexis* may have been the most cursorial mammal of the early Eocene. Among small mammals, however, there may be no clear distinction between cursorial and saltatory habits; some species employ a combination of both locomotor modes. This is true of tragulids (*30, 31*), small forest ruminants of Asia and Africa, which are the closest living analogs of *Diacodexis*. The resemblance of *Diacodexis* to tragulids in limb proportions and body size suggests that it, too, was an adept leaper. It may have used its long tail for balance, as do several living saltatorial mammals (*24, 29*).

The notion that dichobunids are so primitive and short-limbed that, were it not for their characteristic astragalus, they might not be recognized as artiodactyls is prevalent (*3, 5, 32*). *Diacodexis* does not fit this image, however, nor do other dichobunids which, where known, are progressive and cursorially adapted like *Diacodexis*. The skeleton of *Diacodexis* appears to be slightly more specialized than that of *Messelobunodon* and nearly as specialized as those of *Hypertragulus*, *Archaeomeryx*, and *Tragulus*, which are considered to be the most primitive Ruminantia (Tragulina) (*17*). The only important postcranial features which are more primitive in *Diacodexis* than in tragulines are its free proximal fibula, retention of metatarsal I, and separate cuboid and navicular elements in the tarsus. This raises the question of whether *Diacodexis* is representative of the primitive artiodactyl skeletal condition, or whether it is too specialized to be ancestral to Suina and some extinct nonruminant groups. If *Diacodexis* is representative, we must revise our concept of the primitive artiodactyl skeleton and assume that reversal of cursorial trends (toward elongation and lightening of the limbs and reduction in size of some elements) must have occurred in various nonruminant lineages. While such reversals are possible (*33, 34*), it is equally probable, as judged from present evidence, that the basal artiodactyl was an unknown bunodont form with a much more generalized skeleton than that of *Diacodexis*.

KENNETH D. ROSE
Department of Cell Biology and Anatomy, Johns Hopkins University School of Medicine, Baltimore, Maryland 21205

References and Notes

1. G. G. Simpson, *Bull, Am. Mus. Nat. Hist.* **85**, 1 (1945).
2. C. L. Gazin, *Smithson. Misc. Coll.* **128** (No. 8), 1 (1955).
3. A. S. Romer, *Vertebrate Paleontology* (Univ. of Chicago Press, Chicago, 1966).
4. D. A. Guthrie, *J. Mammal.* **49**, 297 (1968).
5. D. J. Golz, *Nat. Hist. Mus. Los Angeles Cty. Sci. Bull.* **26**, 1 (1976).
6. W. J. Sinclair, *Bull. Am. Mus. Nat. Hist.* **33**, 267 (1914).
7. M. C. McKenna, *Univ. Calif. Publ. Geol. Sci.* **37**, 1 (1960).
8. C. L. Gazin, *Smithson. Misc. Coll.* **144** (No. 1), 1 (1962).
9. T. M. Bown, *Geol. Surv. Wyo. Mem.* **2**, 1 (1979).
10. K. D. Rose, *Univ. Mich. Pap. Paleontol.* **26**, 1 (1981).
11. D. M. Schankler, *ibid.* **24**, 99 (1980).
12. M. Godinot, *C. R. Somm. Seances Soc. Geol. Fr.* **6**, 286 (1978).
13. ——, *Palaeovertebrata* **10**, 43 (1981).
14. L. Van Valen, *Evolution* **25**, 523 (1971).
15. J. Viret, in *Traité de Paléontologie*, J. Piveteau, Ed. (Masson, Paris, 1961), vol. 6, p. 887.
16. E. D. Cope, *Rept. U.S. Geol. Surv.* **3**, 1 (1884).
17. S. D. Webb and B. E. Taylor, *Bull. Am. Mus. Nat. Hist.* **167**, 117 (1980).
18. O. C. Marsh, *Am. J. Sci. Arts* **4**, 1 (August 1872).
19. ——, *Am. J. Sci.* **48**, 259 (1894).
20. M. Schlosser, *Morph. Jahrb.* **12**, 1 (1887).
21. J. L. Franzen, *Senckenbergiana Lethaea* **61**, 299 (1981).
22. W. B. Scott, *Trans. Am. Philos. Soc.* **28**, 363 (1940).
23. B. Schaeffer, *Am. Mus. Novit. 1356* (1947).
24. M. Hildebrand, *Analysis of Vertebrate Structure* (Wiley, New York, 1974).
25. L. B. Radinsky, *Evolution* **20**, 408 (1966).
26. E. H. Colbert, *Am. Mus. Novit. 1135* (1941).
27. J. Hürzeler, *Schweiz. Palaeontol. Abh.* **43**, 1 (1936); *ibid.* **44**, 90 (1937).
28. M. R. Thorpe, *Peabody Mus. Nat. Hist. Yale Univ. Mem.* **3** (No. 4), 1 (1937).
29. A. B. Howell, *Speed in Animals* (Hafner, New York, 1944).
30. G. Dubost, *Terre Vie* **1**, 3 (1968).
31. ——, *Z. Tierpsychol.* **37**, 403 (1975).
32. T. A. Vaughan, *Mammalogy* (Saunders, Philadelphia, 1978).
33. R. Lande, *Evolution* **32**, 73 (1978).
34. N. Macbeth, *Syst. Zool.* **29**, 402 (1980).
35. The skeleton of *Diacodexis* was found by M. J. Kraus during U.S. Geological Survey project 1-9590-02705, conducted jointly by T. M. Bown (U.S. Geological Survey) and K.D.R. I thank S. Anderson, R. T. Bakker, T. M. Bown, K. Carpenter, R. J. Emry, M. C. McKenna, and R. Thorington for access to specimens; R. J. Emry, P. D. Gingerich, F. A. Jenkins, Jr., L. B. Radinsky, A. C. Walker, and S. D. Webb for informative discussion and comments on the manuscript; D. Bichell for preparing the illustrations; and T. Urquhart for photography. Support by the J. J. Hopkins Fund of Johns Hopkins University and by the National Geographic Society.

16 December 1981; 12 February 1982

Upwelling of Hydrothermal Solutions Through Ridge Flank Sediments Shown by Pore Water Profiles

Abstract. *High calcium ion and low magnesium ion concentrations in sediment pore waters in cores from the Galápagos Mounds Hydrothermal Field on the flank of the Galápagos Spreading Center are believed to be due to a calcium-magnesium exchange reaction between circulating seawater and basement basalt. The nonlinearity of the calcium ion and magnesium ion gradients indicates that these discharging hydrothermal solutions on the ridge flank are upwelling at the rate of about 1 centimeter per year through the pelagic sediments of the Mounds Field and at about 20 centimeters per year through the hydrothermal mounds themselves.*

The recent discovery of hot springs on the Galápagos Ridge (*1*) and the East Pacific Rise (*2*) has provided the most spectacular evidence of ridge crest convection of seawater through hot basalt. The composition of these samples (*3*), together with earlier evidence (*4*), indicates that seawater-basalt exchange attending hydrothermal circulation is important in the marine mass balances of several elements; the process is a sink for seawater Mg^{2+} and a source of seawater Ca^{2+}. The intense convection of water at the center of spreading appears to cool the entire crust (*5*) but is of short duration, as reflected in the fact that the discharge of high-temperature hydrothermal solutions is limited to young crustal segments (*1*). Convection and associated hydrothermal processes continue at a much slower rate on the ridge flanks, for 5×10^6 to 7×10^7 years (*6*). This ridge flank convection process is reflected by a deficiency in conductive heat flow (*6*), increasing layer-2 velocity (velocity of basalt) (*7*), and nonlinear heat flow profiles indicating upwelling and downwelling of solutions through sediments (*6*). Sleep *et al.* (*8*) have argued that most of the global convective heat loss actually takes place on the ridge flanks.

The southern flank of the Galápagos Spreading Center is now the best understood example of a ridge flank convection system. Heat flow has been mapped in detail to a distance of 30 km south of the center of spreading (*5, 9*) (Fig. 1). The variations are believed to reflect the flow of water through the sediments to

 0036-8075/82/0507-0623$01.00/0

and from the basement aquifer. Low heat flow bands are believed to be sites of downwelling (basement aquifer recharge), and high heat flow zones (> 12 heat flow units) are believed to be sites where hydrothermal solutions are upwelling and discharging. Nonlinear heat flow gradients, reflecting advection, support this interpretation. The high heat flow zone shown in Fig. 1, about 17 km south of the axis, is the site of sediment mounds composed of MnO_2 and nontronite, $Fe_4Si_8O_{20}(OH)_4$, believed to originate from the oxidation of discharging hydrothermal Fe^{2+} and Mn^{2+} (*1, 10, 11*).

We sampled pore waters from pelagic sediments around mounds from cores taken in March 1979 from R.V. *Gillis* and from mounds from D.S.R.V. *Alvin* cores taken in December 1979 by Dr. Fred Grassle of Woods Hole Oceanographic Institution. The composition of the interstitial solutions in the Mounds Hydrothermal Field reflects upwelling of hydrothermal solutions (that is, geothermally warmed, advected waters) whose compositions have been altered by reaction with basalt. The compositions of these solutions reflect seawater-basalt reaction on the ridge flanks and differ greatly from that of ridge crest hydrothermal solutions.

The cores discussed in this study were taken from locations shown in Fig. 1. We separated pore waters from cores by centrifuging at 4°C and filtering through 0.45-μm Nuclepore filters, as well as by in situ sampling (by Dr. Ross Barnes, Walla Walla College Marine Station). The $[Ca^{2+}]$ and $[Mg^{2+}]$ values were measured by EGTA (*12*) and EDTA (*13*) titration, respectively. Chlorinity was analyzed by Mohr titration (*14*) to correct for evaporation. Variations from seawater values are believed to be due entirely to changes in $[Mg^{2+}]$ and $[Ca^{2+}]$ (*15*).

The $[Ca^{2+}]$ and $[Mg^{2+}]$ values in the cores from the low heat flow area are close to those of bottom water (Fig. 2A). The cores from the high heat flow area and the *Alvin* cores have higher $[Ca^{2+}]$, lower $[Mg^{2+}]$, and nonlinear concentration versus depth profiles (Fig. 2, B and C). These anomalies are larger than anomalies arising from in situ diagenesis (*16*) and are believed to reflect Ca^{2+} dissolution and Mg^{2+} uptake attending seawater-basalt exchange in the basement.

The in situ samples should be free of most sampling artifacts. Although the same is not true for the centrifuge samples (*17*), the concentration anomalies in the cores from the high heat flow area cannot reasonably be ascribed to such artifacts. Artifacts cause $[Ca^{2+}]$ to fall by about 3 percent, not to rise (*18*). The $[Mg^{2+}]$ data are more uncertain because the observed decrease (1.5 to 2.0 m*M*) corresponds to a concentration change of only 3 to 4 percent. Our measured Mg^{2+}/Cl^- ratios are higher by up to 2 percent than the bottom water ratios, as in samples PC 30, ISPW 126, PC 28, and PC 29. It is still unknown if this difference is real, is a sampling artifact that also affects the in situ samples, or is due to an unknown divalent cation interfering with the titration. However, there is no reason to doubt the validity of the $[Mg^{2+}]$ decrease in high heat flow cores, although its magnitude is uncertain.

One may model the shape of the Ca^{2+} and Mg^{2+} profiles, if one assumes that the gradients reflect diffusion and advection only, by using the diffusion advection model (*19*). According to a diffusion advection equation for a conservative, nonradioactive species and assuming steady state and constant diffusivity, we find that

$$w\frac{dC}{dz} = D_a\frac{d^2C}{dz^2}$$

where w is the vertical advection rate, C is the concentration of the species of interest, z is the depth in the sediment column (positive upward), and D_a is the apparent diffusion coefficient of the species of interest. The solution of this differential equation is

$$\frac{C - C_0}{C_{max} - C_0} = \frac{e^{z/z^*} - 1}{e^{z_{max}/z^*} - 1}$$

where C_0 is the concentration of the species of interest at $z = 0$ (the sediment-water interface), C_{max} is the asymptotic concentration of the species, z_{max} is the asymptotic depth, and $z^* = D_a/w$.

The shape of the conservative species versus depth profile is dependent on the values of w and z^*. A small value of z^* (advection-dominated transport) will result in a nonlinear gradient, with the degree of curvature related to z^*. A large value of z^* (diffusion-dominated transport) will give a straight line connecting the two end-members. Therefore, given the depth variation of a conservative, nonradioactive species and an experimental value for D_a (*20*), the advection rate can be calculated. Heat flow probes use temperature as the conservative tracer; a concave-down nonlinear temperature gradient is believed to indicate upward advection of warm hydrothermal water (*1, 6, 9*). Similarly, Ca^{2+} and Mg^{2+} gradients can be used as conservative chemical tracers in the Galápagos Mounds Hydrothermal Field.

The advection rates we have calculated from the $[Ca^{2+}]$ values of high heat flow cores average about 1 cm/year (Fig. 2B). Temperature profiles from samples PC 22 and PC 30 are linear, as would be expected for this slow upward advection rate (*21*). Upward advection rates in the region calculated from temperature profiles measured while piston coring in the mounds are about 30 cm/year. Our three

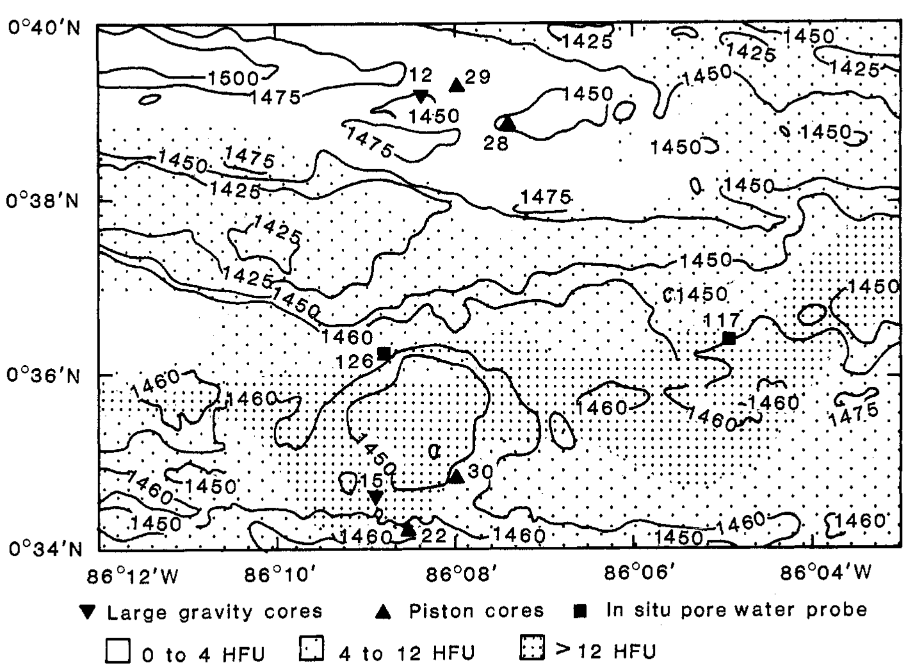

Fig. 1. Map of the study area. The Galápagos Spreading Center is about 20 km north of this area. Contours are depths in fathoms; *HFU*, heat forming units.

Alvin cores were also taken directly through mounds. The advection rates calculated from the [Ca^{2+}] values through mounds are approximately 20 cm/year (Fig. 2C).

The calculated advection rates imply that the mounds themselves act as chimneys for upwelling water (*1, 11, 15*). The flow through the mounds is at least 20 to 30 times more rapid than the slow upward percolation of water in the surrounding sediment. The mounds contain about 10 m of nontronite gravel, which is much less resistant to flow than the surrounding sediments and probably facilitates rapid flow. The mounds generally overlie faults in the basement. These cracks in the basalt are likely places for the venting of hydrothermal water and thus produce more rapid advection rates at the base of the sediment in these areas than at the base of the surrounding sediments. Both effects are probably important in the formation of the hydrothermal

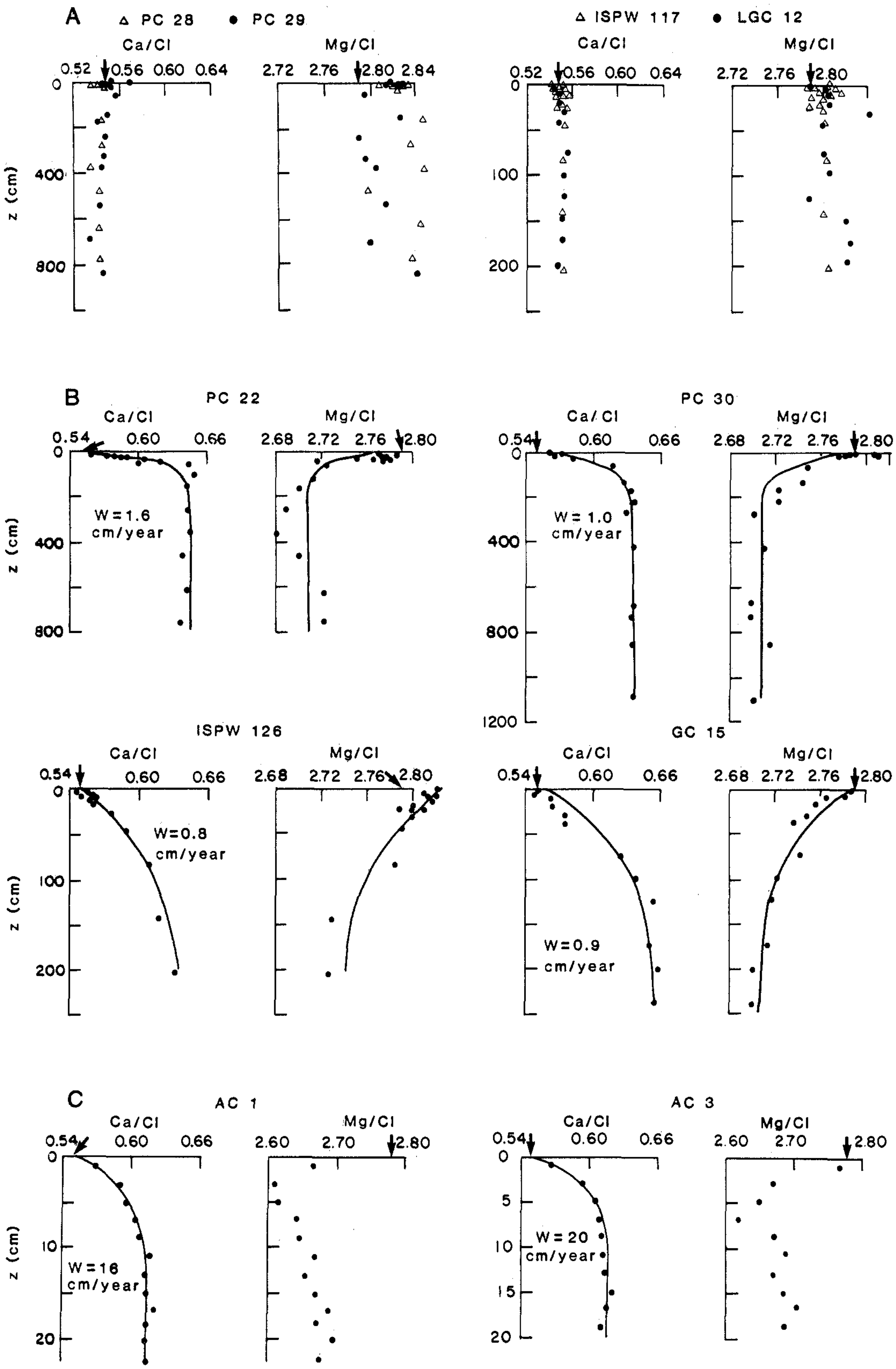

Fig. 2. The [Ca^{2+}] and [Mg^{2+}] values in pore waters from (A) a low heat flow area, (B) a high heat flow area (mounds area), and (C) hydrothermal mounds (sampled by *Alvin*); concentrations for Ca^{2+} and Mg^{2+} are in millimoles per liter, and the Cl^- concentrations are in grams per kilogram. Samples ISPW 117 and 126 were collected with Ross Barnes's in situ pore water sampler. Values in (A) are very close to bottom water values (indicated by arrows). High [Mg^{2+}] values in some pore waters may be sampling artifacts. High asymptotic [Ca^{2+}] and low [Mg^{2+}] values in (B) and (C) are believed to be due to seawater-basalt exchange in the underlying basement. Solid lines are the calculated gradients based on the use of a diffusion advection model and the indicated advection rates (*w*). The advection rates from [Ca^{2+}] values in mounds (C) are 10 to 20 times those of cores taken between mounds (B). The relationship between Ca^{2+} enrichment and Mg^{2+} depletion is not as simple as shown in (B).

mounds. Mounds might form over basement faults, supplying an increased flow of warm water rich in Fe^{2+} and Mn^{2+}. The nontronite gravel formed by these solutions reduces the resistance to flow, thus reinforcing the rapid flow of water through the sediment and possibly facilitating the formation of mounds.

The Ca^{2+} and Mg^{2+} profiles in the Galápagos Hydrothermal Mounds Field provide evidence for convection in sediments independent of heat flow measurements. The nonlinear gradients can be used to calculate upward advection rates of about 1 cm/year through pelagic sediments around mounds. The advection rates calculated from $[Ca^{2+}]$ in mound cores, about 20 to 30 cm/year, are in good agreement with the rates calculated for other mounds from temperature profiles. The data and gradients provide important new information about the extent and importance of ridge flank convection; information on such convection up to now has been confined to geophysical studies. Future work should be directed toward further characterizing the composition of the hydrothermal fluid entering the sediments in this area.

CYNTHIA R. P. MARIS
MICHAEL L. BENDER
Graduate School of Oceanography, University of Rhode Island, Kingston 02881

References and Notes

1. J. B. Corliss *et al.*, *Science* **203**, 1073 (1979).
2. RISE Project Group, *ibid.* **207**, 1421 (1980).
3. J. M. Edmond, C. Measures, R. E. McDuff, L. H. Chan, R. Collier, B. Grant, L. I. Gordon, J. B. Corliss, *Earth Planet. Sci. Lett.* **46**, 1 (1979).
4. J. L. Bischoff and F. W. Dickson, *ibid.* **25**, 385 (1975); M. J. Mottl and H. D. Holland, *Geochim. Cosmochim. Acta* **42**, 1103 (1978).
5. K. Green, thesis, Massachusetts Institute of Technology–Woods Hole Oceanographic Institution (1980).
6. R. N. Anderson, M. G. Langseth, J. G. Sclater, *J. Geophys. Res.* **82**, 3391 (1977); R. N. Anderson, M. A. Hobart, M. G. Langseth, *Science* **204**, 828 (1979).
7. R. Houtz and J. Ewing, *J. Geophys. Res.* **81**, 2490 (1976).
8. N. H. Sleep, J. Morton, L. Gagnon, *Eos* **61**, 99 (1980).
9. D. L. Williams, R. P. Von Herzen, J. G. Sclater, R. N. Anderson, *Geophys. J. R. Astron. Soc.* **38**, 587 (1974); D. L. Williams, K. Green, T. Van Andel, R. Von Herzen, J. Dymond, K. Crane, *J. Geophys. Res.* **84**, 7467 (1979).
10. P. Lonsdale, *Earth Planet. Sci. Lett.* **36**, 92 (1977).
11. J. B. Corliss, M. Lyle, J. Dymond, K. Crane, *ibid.* **40**, 12 (1978).
12. J. M. Gieskes, *Init. Rep. Deep Sea Drill. Proj.* **20**, 813 (1973).
13. The Mg technique was modified slightly. No butanol extractant or trace-metal complexing agents were used.
14. J. D. H. Strickland and T. R. Parsons, *Fish. Res. Board Can. Bull.* **167**, 11 (1968). The technique was modified to use only 0.100 ml of solution, and a microburet was used for the titration.
15. Chloride may not be totally conservative in hydrothermal systems. However, variations in the Galápagos Ridge crest chlorinity data are only about ±0.2 per mil, which would not seriously affect our Ca^{2+}/Cl^- or Mg^{2+}/Cl^- ratios (*3*).
16. F. L. Sayles, *Geochim. Cosmochim. Acta* **43**, 527 (1979).
17. J. L. Bischoff, R. E. Greer, A. O. Luistro, *Science* **167**, 1245 (1970).
18. S. Emerson, personal communication; M. Bender, unpublished data.
19. H. Craig, *J. Geophys. Res.* **74**, 5491 (1969); J. D. Bredehoeft and I. S. Papadoupulos, *Water Resour. Res.* **1**, 325 (1965).
20. Y. H. Li and S. Gregory, *Geochim. Cosmochim. Acta* **38**, 703 (1974).
21. K. Becker and R. P. Von Herzen, in preparation.
22. We thank the officers, scientists, and crew of R.V. *Gillis* cruise 7901, Leg III, especially J. Edmond, J. Corliss, P. Froelich, P. Tropeano, D. Lanesky, and N. Luedtke. We also acknowledge the essential collaboration of R. Von Herzen and K. Becker, who carried out heat flow studies. Supported by NSF grant OCE-7921137.

26 October 1981; revised 12 January 1982

Blade Technology in the Egyptian Nile Valley: Some New Evidence

Abstract. *An Upper Paleolithic site with blade technology was excavated at Nazlet Khater, Egypt. Radiocarbon dates center around 31,500 years ago, indicating that the Egyptian Nile Valley was not an isolated enclave where blade technology appeared late in comparison with other eastern Mediterranean areas. This site fills a gap in the record of human history in Egypt between 40,000 and 20,000 years ago.*

In the Egyptian Nile Valley, blade industries of Upper Paleolithic style are known from many sites that were excavated by the Combined Prehistoric Expedition (*1, 2*). The investigators correlated these industries with a period of Nile aggradation that, on the basis of numerous radiocarbon dates, occurred less than 19,000 years ago. With the reassessment of the Nubian chronology (*3, 4*), the Khormusan industry, originally estimated to date between 27,000 and 18,000 years ago, is now considered to be much older, possibly dating back more than 40,000 years. This is more consistent with the Middle Paleolithic features of the Khormusan industry, but the new chronology implies that there is a gap of more than 20,000 years in our knowledge of the record of human history in the lower Nile Valley. Indeed, no archeological complexes or Nile sediments have been placed with any confidence within this interval (*2*). The excavations of the Belgian Middle Egypt Prehistoric Project at Nazlet Khater near Tahta in Upper Egypt (*5, 6*) have now provided evidence of the presence of blade-producing communities within this interval along the Nile.

During the past 4 years four sites were excavated in the lower desert of Nazlet Khater (Fig. 1). This lower desert is that part of the desert which belongs to the Nile Valley. Nazlet Khater 1 is situated on a small elevation adjacent to the edge of the cultivated zone. Nile sediments—gravels, silts, and clays—form the core of this elevation. The uppermost gravel deposit, of Nilotic origin, which is 5 m above the alluvial plain and partially covered by Nile silts, contains numerous Middle Paleolithic artifacts. The upper part of the elevation, consisting of local wadi-slope deposits, is rich in artifacts (more than 1000 per square meter) that are also of Middle Paleolithic age. The differences between the industries repre-

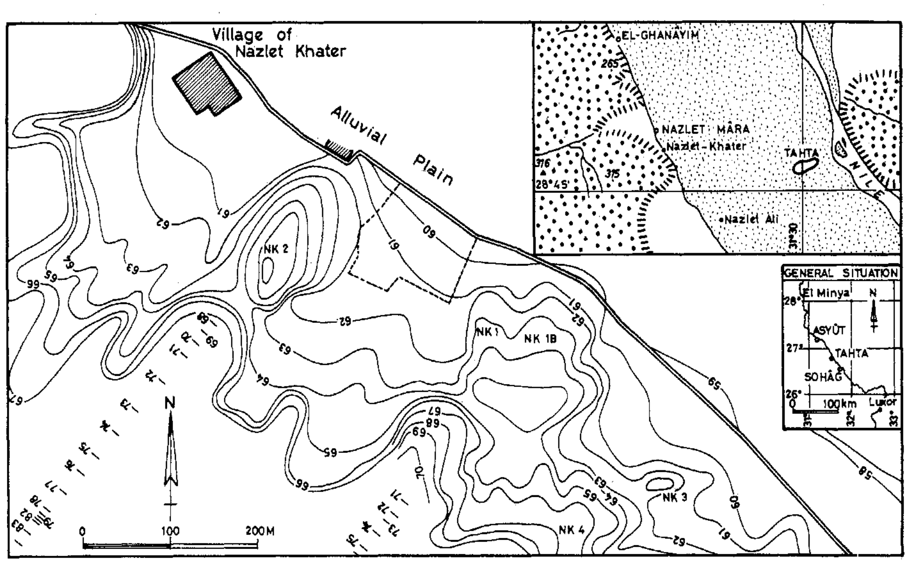

Fig. 1. Topographic map of the area in the vicinity of the modern village of Nazlet Khater and the Paleolithic sites of Nazlet Khater (*NK*) 1, 1B, 2, 3, and 4. The contour lines are in meters.